2023-01-19

Dynamic modelling and optimal control analysis of a fractional order chikungunya disease model with temperature effects

Lusekelo, Eva

Dynamic modelling and optimal control analysis of a fractional order chikungunya disease model with temperature effects

Eva Lusekelo [a,b], Mlyashimbi Helikumi [c], Dmitry Kuznetsov [a], Steady Mushayabasa [d,*]

[a] School of Computational and Communication Science and Engineering, The Nelson Mandela African Institution of Science and Technology, P.O. Box 447, Arusha, Tanzania
[b] Department of Mathematics, College of Natural and Mathematical Sciences, University of Dodoma, Dodoma, Tanzania
[c] Mbeya University of Science and Technology, Department of Mathematics and Statistics, College of Science and Technical Education, P.O. Box 131, Mbeya, Tanzania
[d] University of Zimbabwe, Department of Mathematics and Computational Sciences, P.O. Box MP 167, 630 Churchill Avenue, Mount Pleasant, Harare, Zimbabwe

ARTICLE INFO

ABSTRACT

Approximately 1.3 billion inhabitants in 94 countries are estimated to be at risk of chikungunya virus infection. A mechanistic compartmental model based on fractional calculus, the Caputo derivative has been proposed to evaluate the effects of temperature and multiple disease control measures (larvicides use, insecticides and physical barriers) during an outbreak. The proposed model was calibrated based on data from literature and validated with daily chikungunya fever cases reported at Kadmat primary health centre, India. The transmission potential of the disease was examined. Sensitive analyses were conducted through computing partial rank correlation coefficients. Memory effects which are often neglected when mechanistic models are used to model the transmission dynamics of infectious diseases, were found to have a significant effect on the dynamics of chikungunya.

1. Introduction

In recent years, Chikungunya, a mosquito-borne viral disease has spread globally and invaded new habitats and as such, it is now regarded as one of the global threat to humanity because of its highly debilitating nature and unprecedented magnitude of its spread [1]. Although CHIKV outbreaks occurs throughout the tropical and subtropical regions of the world, intra-annual patterns of human infections vary geographically [2]. According to the World Health Organization (WHO), about 1.3 billion inhabitants in 94 countries are at risk to Chikungunya virus (CHIKV) infection [1]. The recent increase in CHIKV outbreaks calls for extensive research that focuses on understanding the impacts of deploying various disease control strategies during an outbreak.

Various approaches can be used to investigate the impacts of deploying single or multiple intervention strategies during a CHIKV outbreak, however, in recent years, mathematical models have proved to be useful tools capable of guiding policy makers and epidemiologists on when and how to deploy intervention strategies in order to minimize the spread of infectious diseases. As such, a couple of mathematical models for CHIKV transmission have been developed recently, aimed at studying the impacts of: temperature [3–6], temperature and heterogeneous biting exposure of the host [7], temperature and human mobility [8], seasonal variations [9] and intervention strategies [10,11].

As efforts to understand the impacts of deploying interventions during a CHIKV outbreak continue, there remains significant gaps in understanding the joint impacts and cost of implementing these interventions. One of the limitations in prior CHIKV studies, is

that most of the models proposed to characterize the joint impacts and cost of deploying single or multiple interventions during an outbreak are based on integer ordinary differential equations, despite growing evidence that integer ordinary differential equations are not capable of capturing memory effects which are inherent in many biological processes [10,12–16]. On the other hand, use of fractional order derivatives to model biological process has gained popularity recently, due to their ability to capture memory effects [10,16]. To this end, in the present study, we propose a fractional order CHIKV transmission model that incorporates temperature effects and three interventions (larvicide use, insecticides use and use of physical barriers), with a goal to investigate the joint impacts and costs associated with deployment of these strategies during an outbreak.

Although several types of fractional derivatives exist in literature, our model is based on the Caputo derivative. The choice of using the Caputo derivative was motivated by the following merits: (i) the Caputo derivative for a given function which is constant is zero, this is the same result for integer ordinary differential equations; (ii) the Caputo operator computes an ordinary differential equation, followed by a fractional integral to obtain the desired order of fractional derivative, and (iii) the Caputo fractional derivative allows the use of local initial conditions to be included in the derivation of the model [10]. The effects of temperature were incorporated by modelling all entomological parameters sensitive to environmental changes as function of temperature.

The remaining part of this paper is organized as follows: Section 2 contains the dynamical analysis of the basic model. In particular, we developed a new mathematical model for CHIKV transmission, derived the reproduction number and explored the effects of temperature and three control strategies; larvicide use, insecticide and physical barrier for disease severity. In Section 3, we perform an optimal control study to determine the implications of time-dependent insecticide, larvicide and physical barrier on minimizing the number of infectious humans over time at minimal costs. The formulated optimal control problem is explored analytically and numerically. The paper is concluded in Section 4.

2. Mathematical model of chikungunya fever

2.1. Model derivation

We stratify the host population (humans) into five mutually exclusive health states: susceptible $S_h(t)$, latent $E_h(t)$, infectious symptomatic, $I_{hs}(t)$, infectious asymptomatic $I_{ha}(t)$, and recovered with lifelong immunity $R_h(t)$. Thus, the total human population at time t is: $N_h(t) = S_h(t) + E_h(t) + I_{hs}(t) + I_{ha}(t) + R_h(t)$. Since the dynamics of the disease are being explored over a short duration (an outbreak is at most one year), we ignore birth and natural death rates of the host population and assume that the total population is constant, $N_h(t) = N_h$. The life cycle of mosquitoes is divided into aquatic $A_v(t)$ (including eggs, larvae and pupaes) and adult $N_v(t)$ stages. The adult population is further subdivided into susceptible $S_v(t)$, latent $E_v(t)$ and infectious $I_v(t)$ stages, such that $N_v(t) = S_v(t) + E_v(t) + I_v(t)$. The life cycle of mosquitoes begins with the aquatic stages where recruitment is assumed to occur at per capita rate:

$$f(A_v, N_v) = \theta_v \left(1 - \frac{A_v}{K_v} \right) N_v. \tag{1}$$

In (1), K_v represents the maximum population of the mosquito in the aquatic stage the environment can support also known as the aquatic environment carrying capacity, θ_v is the intrinsic oviposition rate of adult mosquitoes. The population of mosquitoes in the aquatic stage reduces due to natural mortality rate d_v, transition to adult stage at the rate ϕ_v, and vector-control measures such as larvicide spraying at the rate u_1. Disease transmission between the host and vector is assumed to occur only when a susceptible mosquito takes a blood meal from an infectious human or an infectious mosquito takes a blood meal from an susceptible host. Susceptible vectors are infected with CHIKV following a blood meal from an infectious individual at the rate:

$$\lambda_v(t) = \frac{b_v \beta_h (1 - u_2)(I_{hs} + I_{ha})}{N_h}. \tag{2}$$

In (2), β_h denotes the probability of infection transmission from an infectious host to a susceptible vector and $0 \leq u_2 < 1$ account for the reduction in the biting rate of mosquitoes due to use of the preventative strategies such as insecticide-treated bed nets (ITNs). Upon exposure to CHIKV, vectors incubate the disease for $1/\alpha_v$ days, after which they become infectious for their entire life span. It is also assumed that the adult vector population reduces at the rate u_3 in all the epidemiological stages due to insecticide use. Upon being bitten by an infectious vector, a susceptible individual is assumed to acquire infection at the rate

$$\lambda_h(t) = \frac{b_v \beta_v (1 - u_2) I_v}{N_h}. \tag{3}$$

In (3), β_v is the probability that an infectious vector successfully transmits the virus while taking a blood meal from a susceptible human. Once exposed to CHIKV infection, the host incubates the disease for a duration $1/\alpha_h$ days, after which a proportion f_h become asymptomatic infectious patients and the remainder, $(1 - f_h)$, becomes symptomatic infectious patients. The average infectious period for symptomatic infectious individuals is $1/\gamma_h$ days, and asymptomatic infectious individuals are assumed to be infectious for an average period of $1/\delta_h$ days. Recovered individuals are assumed to gain permanent immunity [17].

The transmission dynamics of CHIKV under the above assumptions are summarized by the following differential equations (Model flow diagram is in Fig. 1):

$$
\left.
\begin{aligned}
{}_{b}^{c}D_{t}^{q}A_{v}(t) &= f(A_{v}(t), N_{v}(t)) - (\phi_{v} + u_{1} + d_{v})A_{v}(t), \\
{}_{b}^{c}D_{t}^{q}S_{v}(t) &= \phi_{v}A_{v}(t) - \lambda_{v}(t)S_{v}(t) - (u_{3} + \mu_{v}^{q})S_{v}(t), \\
{}_{b}^{c}D_{t}^{q}E_{v}(t) &= \lambda_{v}(t)S_{v}(t) - (\alpha_{v} + u_{3} + \mu_{v}^{q})E_{v}(t), \\
{}_{b}^{c}D_{t}^{q}I_{v}(t) &= \alpha_{v}E_{v}(t) - (u_{3} + \mu_{v})I_{v}(t), \\
{}_{b}^{c}D_{t}^{q}S_{h}(t) &= -\lambda_{h}(t)S_{h}(t), \\
{}_{b}^{c}D_{t}^{q}E_{h}(t) &= \lambda_{h}(t)S_{h}(t) - \alpha_{h}E_{h}(t), \\
{}_{b}^{c}D_{t}^{q}I_{hs}(t) &= (1 - f_{h})\alpha_{h}E_{h}(t) - \gamma_{h}I_{hs}(t), \\
{}_{b}^{c}D_{t}^{q}I_{ha}(t) &= f_{h}\alpha_{h}E_{h}(t) - \delta_{h}I_{ha}(t), \\
{}_{b}^{c}D_{t}^{q}R_{h}(t) &= \gamma_{h}I_{hs}(t) + \delta_{h}I_{ha}(t),
\end{aligned}
\right\}
\tag{4}
$$

and the following initial conditions:

$$
\left.
\begin{aligned}
S_{h}(0) &= S_{h0}, & E_{h}(0) &= E_{h0}, & I_{hs}(0) &= I_{hs0}, & I_{ha}(0) &= I_{ha0}, & R_{h}(0) &= R_{h0}, \\
A_{v}(0) &= A_{v0}, & S_{v}(0) &= S_{v0}, & E_{v}(0) &= E_{v0}, & I_{v}(0) &= I_{v0}.
\end{aligned}
\right\}
$$

Model (4) is based on the Caputo fractional derivative [18] and $q \in (0, 1]$ represent the order of the fractional derivative. For $q = 1$, model (4) becomes the integer ordinary differential equation system. The Caputo fractional derivative is defined by:

$$
{}_{b}^{c}D_{t}^{q}f(t) = \frac{1}{\Gamma(n-q)} \int_{0}^{t} (t-\xi)^{n-q-1} f^{n}(\xi)d\xi, \quad n-1 < q < n \in \mathbb{N},
\tag{5}
$$

where Γ represents the gamma function [18]. The Riemann Liouville fractional integral of an arbitrary real order $q > 0$ of a function $f(t)$ is defined by :

$$
J^{q}f(t) = \frac{1}{\Gamma(q)} \int_{0}^{t} (t-\xi)^{q-1} f(\xi)d\xi.
\tag{6}
$$

Model (4) exhibits some problems in what concerns time dimension between left and right-hand sides of the equations. On the left, the dimension is $(time)^{-q}$, whereas on the right-hand side the dimension is $(time)^{-1}$. The corrected system corresponding to model (4) is as follows:

$$
\left.
\begin{aligned}
{}_{b}^{c}D_{t}^{q}A_{v}(t) &= f(A_{v}(t), N_{v}(t)) - (\phi_{v}^{q} + u_{1}^{q} + d_{v}^{q})A_{v}(t), \\
{}_{b}^{c}D_{t}^{q}S_{v}(t) &= \phi_{v}^{q}A_{v}(t) - \lambda_{v}(t)S_{v}(t) - (u_{3}^{q} + \mu_{v}^{q})S_{v}(t), \\
{}_{b}^{c}D_{t}^{q}E_{v}(t) &= \lambda_{v}(t)S_{v}(t) - (\alpha_{v}^{q} + u_{3}^{q} + \mu_{v}^{q})E_{v}(t), \\
{}_{b}^{c}D_{t}^{q}I_{v}(t) &= \alpha_{v}^{q}E_{v}(t) - (u_{3}^{q} + \mu_{v}^{q})I_{v}(t), \\
{}_{b}^{c}D_{t}^{q}S_{h}(t) &= -\lambda_{h}(t)S_{h}(t), \\
{}_{b}^{c}D_{t}^{q}E_{h}(t) &= \lambda_{h}(t)S_{h}(t) - \alpha_{h}^{q}E_{h}(t), \\
{}_{b}^{c}D_{t}^{q}I_{hs}(t) &= (1 - f_{h})\alpha_{h}^{q}E_{h}(t) - \gamma_{h}^{q}I_{hs}(t), \\
{}_{b}^{c}D_{t}^{q}I_{ha}(t) &= f_{h}\alpha_{h}^{q}E_{h}(t) - \delta_{h}^{q}I_{ha}(t), \\
{}_{b}^{c}D_{t}^{q}R_{h}(t) &= \gamma_{h}^{q}I_{hs}(t) + \delta_{h}^{q}I_{ha}(t),
\end{aligned}
\right\}
\tag{7}
$$

2.2. Temperature-dependent model parameters

Based on the observation from laboratory studies, it was noted that entomological parameters are sensitive to temperature, hence they can be modelled with functions of temperature [6,19–21]. To incorporate this aspect, we made use of the experimental results from laboratory studies and define entomological parameters as temperature-dependent, as follows:

(i) The average blood meal frequency of female *Ae. aegypti* mosquitoes linearly increases with increasing temperature per day and can be modelled by the function [6]:

$$
b_{v}(T) = 0.0943 + 0.0043T, \qquad (21\ ^{\circ}\text{C} \leq T \leq 32\ ^{\circ}\text{C}).
$$

(ii) The probability of transmission of the CHIKV from an infected human to a susceptible mosquito is [20]:

$$
\beta_{h} = \begin{cases} 0.0729T - 0.9037, & 12.4\ ^{\circ}\text{C} \leq T \leq 26.1\ ^{\circ}\text{C} \\ 1, & 26.1\ ^{\circ}\text{C} < T \leq 32.5\ ^{\circ}\text{C} \end{cases}
$$

(iii) The probability of transmission of CHIKV from an infected mosquito to a susceptible host is [20]:

$$
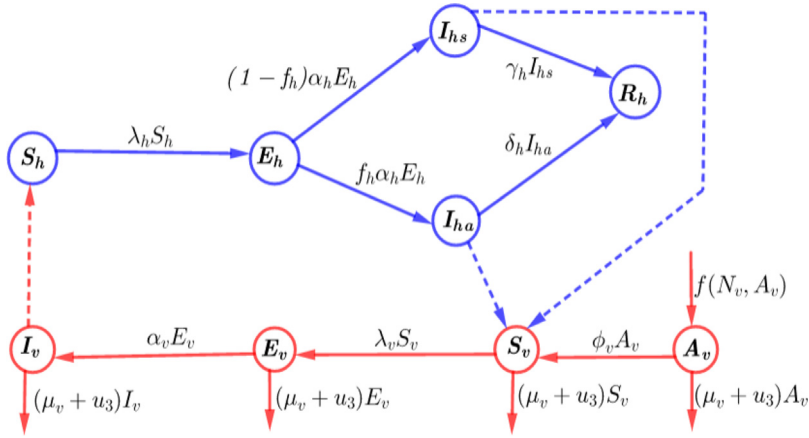\beta_{v}(T) = 0.001T(T - 12.286)\sqrt{32.461 - T}.
$$

Fig. 1. Flow diagram on the dynamical transmission of CHIKV between the host and vector.

(iv) The extrinsic incubation period of *Ae. aegypti* mosquitoes can be modelled by the function [21]:

$$\alpha_v^{-1} = 4 + \exp(5.15 - 0.123T).$$

(v) The mortality rate of *Ae. aegypti* mosquitoes satisfied the function [19]:

$$\mu_v(T) = 0.8692 - 0.1590T + 0.01116T^2 - 3.408 \times 10^{-4}T^3 + 3.809 \times 10^{-6}T^4.$$

(vi) The intrinsic oviposition rate of adult mosquitoes is [8]:

$$\theta_v(T) = (-5.4 + 1.8T - 0.2124T^2 + 0.01015T^3 - 1.515 \times 10^{-4}T^4)/7.$$

(vii) Prior studies have demonstrated that the aquatic transition rate to adult stage satisfies the function [8]:

$$\phi_v(T) = (0.131 - 0.05723T + 0.01164T^2 - 0.001341T^3 + 8.723 \times 10^{-5}T^4$$
$$- 3.017 \times 10^{-6}T^5 + 5.153 \times 10^{-8}T^6 - 3.42 \times 10^{-10}T^7)/7.$$

(viii) Prior studies have demonstrated that the mortality rate of aquatic of *Ae. aegypti* mosquitoes satisfy [8]:

$$d_v(T) = (2.13 - 0.3787T + 0.02457T^2 - 6.778 \times 10^{-4}T^3 + 6.794 \times 10^{-6}T^4)/7.$$

2.3. Transmission potential

The basic reproduction number R_0, is commonly used to quantify the potential of the disease to invade the host population during an outbreak. If $R_0 < 1$, it implies that the diseases dies out and $R_0 > 1$ implies that the disease persists. In order to compute R_0 of model (7), one needs to first determine the disease-free equilibrium $\mathcal{E}^0$. Direct calculations shows that the disease-free equilibrium of model (7) is given by $\mathcal{E}^0 = (A_v^0, S_v^0, 0, 0, N_h, 0, 0, 0)$ with

$$
\left.
\begin{aligned}
A_v^0 &= \frac{K_v^q(\phi_v^q + u_1^q + d_v^q)(\mu_v^q + u_3^q)}{\theta_v^q \phi_v^q} \left[\frac{\theta_v^q \phi_v^q}{(\phi_v^q + d_v^q + u_1^q)(\mu_v^q + u_3^q)} - 1 \right], \\
S_v^0 &= \frac{K_v^q(\phi_v^q + u_1^q + d_v^q)}{\theta_v^q} \left[\frac{\theta_v^q \phi_v^q}{(\phi_v^q + d_v^q + u_1^q)(\mu_v^q + u_3^q)} - 1 \right].
\end{aligned}
\right\}
\tag{8}
$$

From (8), one can observe that $\mathcal{E}^0$ exists whenever $r = \frac{\theta_v^q \phi_v^q}{(\mu_v^q + u_3^q)(\phi_v^q + d_v^q + u_1^q)}$, is greater than unity ($r > 1$) otherwise the vector population becomes extinct. The threshold quantity r can be defined as the probability of mosquitoes to survive the aquatic stage $\frac{\phi_v^q}{(\phi_v^q + d_v^q + u_1^q)}$, multiplied by the surviving population of mosquitoes $\frac{\theta_v^q}{(\mu_v^q + u_3^q)}$. Further, analysis reveals that $\mathcal{E}^0$ makes biological sense whenever $\theta_v^q > (\mu_v^q + u_3^q)\left[1 + \frac{d_v^q + u_1^q}{\phi_v^q}\right]$.

Although several methods can be used to derive R_0, one of the commonly method used in the next-generation matrix (NGM) approach in [22]. By closely following the NGM, the nonnegative matrix F that denotes the generation of new infection terms and

Table 1

Baseline values for model parameters used in the model system (7).

Biological description	Symbol	Baseline value	Source
Host incubation period	$1/\alpha_h$	5 (5–12) Days	[27]
Vector biting rate	b_v	0.58 (0.33–1) Day^{-1}	Fitting
Fraction of asymptomatic infectious hosts	f_h	0.1 (0.1–0.3)	[27]
Infectious period of symptomatic hosts	$1/\gamma_h$	10(7–10) Days	[27]
Infectious period of asymptomatic hosts	$1/\delta_h$	10(7–10) Days	[27]
Probability of infection transmission from host to the vector	β_h	0.2549	Fitting
Probability of infection transmission from vector to the host	β_v	0.1356	Fitting
Life span of adult mosquitoes	$1/\mu_v$	30(4–30) Days	[27]
Incubation period of vector	$1/\alpha_v$	7(2–7) Days	[27]
Oviposition rate	θ_v	0.7428 Day^{-1}	See text
Aquatic transition to adult stage	ϕ_v	0.0172 Day^{-1}	See text
Mortality rate of aquatic vectors	d_v	0.0051 Day^{-1}	See text
Aquatic environment carrying capacity	K_v	$10^5(2 \times 10^5 - 10^5)$	Estimate
Larvicide use	u_1	$1.5 \times 10^{-4}(0-1)$ Day^{-1}	Fitting
Physical barrier	u_2	0.518 (0–1)	Fitting
Insecticides use	u_3	$4.6 \times 10^{-4}(0-1)$ Day^{-1}	Fitting
Basic reproduction number	$\mathcal{R}_0$	2.39(1.5 − 7)	Computed

the non-singular matrix V that denotes the remaining transfer terms are respectively given (at the disease-free equilibrium) by

$$F = \begin{bmatrix} 0 & 0 & 0 & \frac{b_v\beta_h S_v^0}{N_h} & \frac{b_v\beta_h S_v^0}{N_h} \\ 0 & 0 & 0 & 0 & 0 \\ 0 & b_v\beta_h & 0 & 0 & 0 \\ 0 & 0 & 0 & 0 & 0 \\ 0 & 0 & 0 & 0 & 0 \end{bmatrix}, \quad V = \begin{bmatrix} \alpha_v + \mu_v & 0 & 0 & 0 & 0 \\ -\alpha_v & \mu_v & 0 & 0 & 0 \\ 0 & 0 & \alpha_h & 0 & 0 \\ 0 & 0 & -(1-f_h)\alpha_h & \gamma_h & 0 \\ 0 & 0 & -f_h\alpha_h & 0 & \delta_h \end{bmatrix}. \tag{9}$$

From (9), it follows that reproduction number of model (4)

$$R_0 = \sqrt{\frac{b_v^{2q}(1-u_2)^2\beta_v\beta_h}{(\mu_v^q+u_3^q)N_h} \frac{\alpha_v^q}{(\alpha_v^q+\mu_v^q+u_3^q)} \frac{K_v}{\theta_v^q(\phi_v^q+d_v^q+u_1^q)(\mu_v^q+u_3^q)^2}\left(r-1\right)\left(\frac{1-f_h}{\gamma_h^q}+\frac{f_h}{\delta_h^q}\right)}. \tag{10}$$

2.4. Estimation of parameter values

To estimate model parameters, we used the 2007 CHIKV outbreak data for Kadmat, India collected over 60 days [23]. The fitting process in this study was performed using the least squares method and Nelder–Mead algorithm [24–26]. In particular, we considered the cumulative clinically infected population I_{hs} over 60 days and computed the root-mean square error (RMSE) as follows:

$$\text{RMSE} = \sqrt{\frac{1}{n}\sum_{k=1}^{60}(I_{hs}(k) - \hat{I}_{hs}(k))^2}. \tag{11}$$

In (11), I_{hs} and $\hat{I}_{hs}$ denote the model estimate and the real data, respectively. On performing the fitting process, we set the total human population to $N_h = 5400$, $I_{hs}(0) = 13$, (the initial number of cases recorded on 2 July 2007); $E_h(0) = I_{ha}(0) = R_h(0) = 0$, $S_h(0) = N_h(0) - I_{hs}(0)$, $N_v = 20{,}000$, $E_v(0) = 500$, $I_v(0) = 500$, $S_v(0) = N_v - E_v(0) - I_v(0)$. During the fitting process, we varied temperature from 23.6 °C to 32.5 to determine the lower and upper bounds for each of the temperature-dependent parameters. The baseline values for other model parameters are in Table 1.

Fig. 2 illustrates the RMSE for different derivative orders. From the illustration, the minimum error of estimation for the given data occurs for $q = 0.94$. Therefore according to this illustration, the best fit is obtained by setting $q = 0.94$. Fig. 3(a) shows the model estimates for $q = 0.94$. In Fig. 3(b), the prediction ability between the integer and fractional models is investigated. It is evident that the estimates for the integer model are close to the real data for the first 30 days thereafter, the estimates significantly deviate from the reported cases compared to the estimates of the fractional-order model. Hence, we conclude that the fractional derivative presents better forecasts compared to the integer model.

2.5. Sensitivity analysis

We used Partial rank correlation coefficient (PRCC) to investigate the relationship between R_0 and the model parameters [28,29]. The PRCC technique makes use of the Latin Hypercube Sampling method, to generate 1000 parameter combinations with each parameter uniformly distributed in its range in Table 1. Model parameters with $PRCCs > 0$ are positively correlated to R_0, that is., whenever they are increased R_0 increases those with $PRCCs < 0$ are negatively correlated to R_0, that is., whenever they are
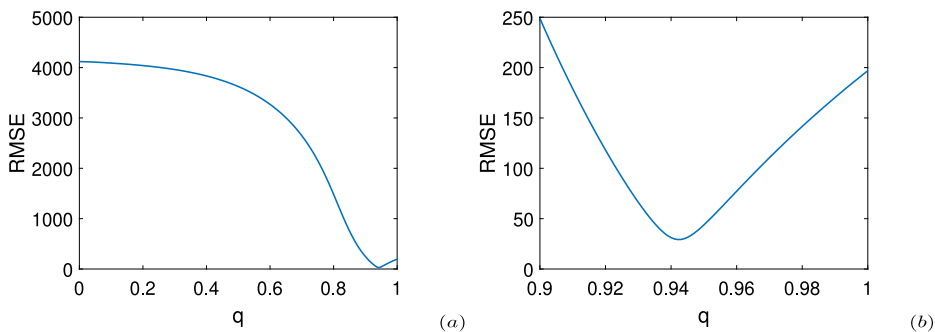
Fig. 2. The RMSE for different derivative orders. In (a) a more wider range of q is considered and in (b) we refined the range of q to improve precision on determining the minimum error of estimation which we observed to occur when $q = 0.94$.
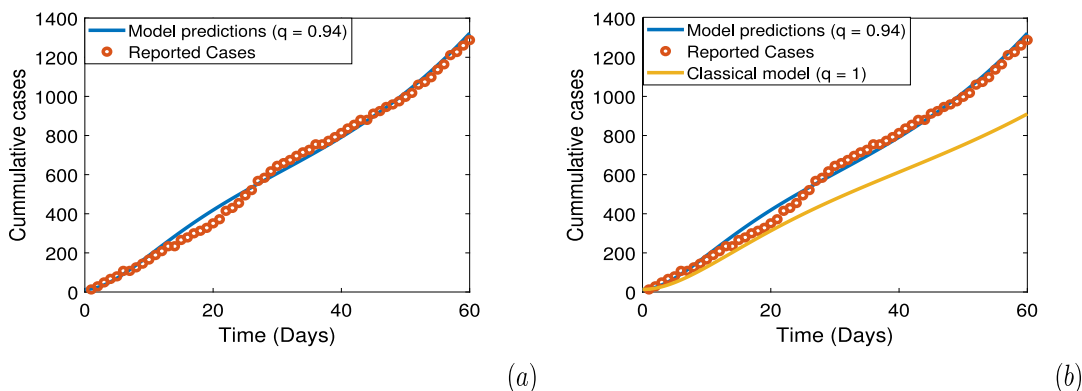

Fig. 3. Data of daily reported CHIKV fever cases at Kadmat primary health centre from 2 July to 7 September 2007 and the model estimation. (a) The estimation of the fractional-order model with $q = 0.94$. (b) Prediction of the fractional-order (with $q = 0.945$) and integer model.
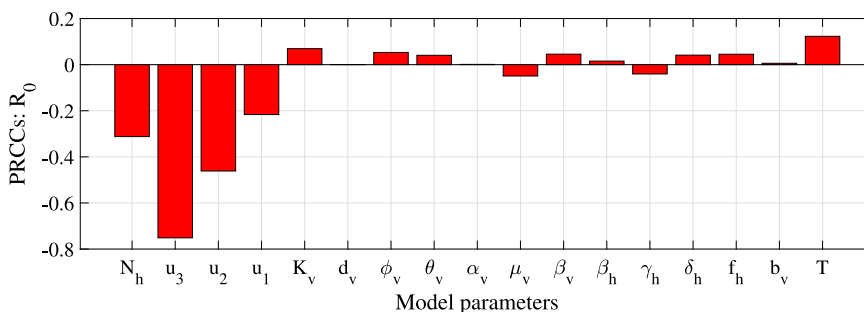
Fig. 4. Global sensitivity analysis of R_0 to key model parameters.

increased R_0, decreases (Fig. 4). A large PRCC indicates that the model parameter has a strong influence to change R_0 whenever it is altered.

Simulation results in Fig. 4 shows that all proposed intervention strategies are significantly negatively correlated to R_0, thus an increase in the intensity of these intervention strategies will reduce the size of R_0. In particular, an increase in larvicide use u_1, by 10% will reduce R_0 by 2%, increasing use of physical barriers u_2, by 10% will reduce R_0 by 4.6% and increasing use of insecticides u_3, by 10% will reduce R_0 by 7.8%.
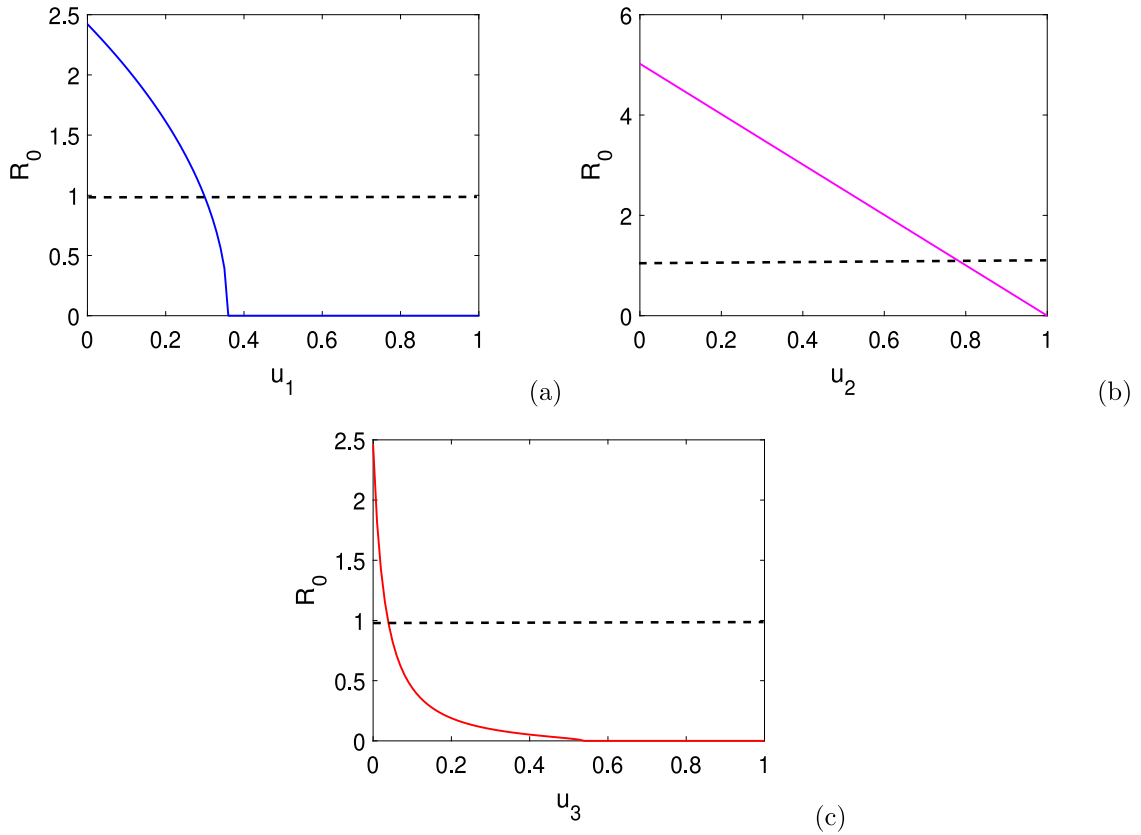
Fig. 5. The relationship between the reproduction number R_0 and disease control strategies, u_i, $i = 1, 2, 3$. Here, one control parameter is varied while other are assume baseline values in Table 1.

2.6. Effects of control strategies on disease persistence

In this section, we characterized the effects of three disease control strategies (larvicide spraying u_1, physical barriers u_2 and insecticides u_3) on R_0 (Figs. 5 and 6) and the population level effects (Figs. 7, 8 and 9).

Simulation results in Fig. 5 shows that (a) an increase in larvicide use to a threshold value greater than 0.3 per day will lead to disease extinction; (b) at least 80% usage of physical barriers all the time will lead to disease to extinction; (c) an increase in use of insecticide to a threshold value greater than 0.1 per day will eliminate the disease from the community during an outbreak.

Contour plots in Fig. 6 shows the transmission potential of CHIKV whenever a combination of two intervention are varied and the third one is fixed. In Fig. 6(a) we observe that increasing larvicide use to a threshold value of 0.3 per day coupled with 60% usage of physical barriers all the time will lead to disease extinction. In Fig. 6(b) we note that increasing larvicide use to a threshold value of 0.4 per day coupled with a minimum usage of insecticide of 0.1 per day will lead to disease extinction. In Fig. 6(c) one can observe that increasing insecticide use to a threshold value of 0.1 per day coupled with 70% usage of physical barriers all the time will lead to disease extinction. Overall, we observed that whenever use of insecticide is increased beyond a rate of 0.3 per day then the number of secondary infections to be generated will be significantly reduced and in some scenarios elimination will be achieved.

Implications of low and high intensity of the control strategies on population level effects were investigated in Figs. 7, 8 and 9. In all scenarios, one can observe that as the intensity of control strategies increases few cases are observed over time.

2.7. Role of memory effects on CHIKV transmission dynamics

Recent studies have shown that memory effects which are inherent in many real-world phenomena including biological problems cannot be fully captured if modellers utilize integer differential equations to analyse the problem. Hence use of fractional calculus to model biological processes has increased recently [10]. To characterize the role of memory effects on CHIKV transmission, we simulated model (7) at different fractional order values $q = \{0.7, 0.8, 0.94, 1.0\}$ and the results are presented in Fig. 10. Simulation
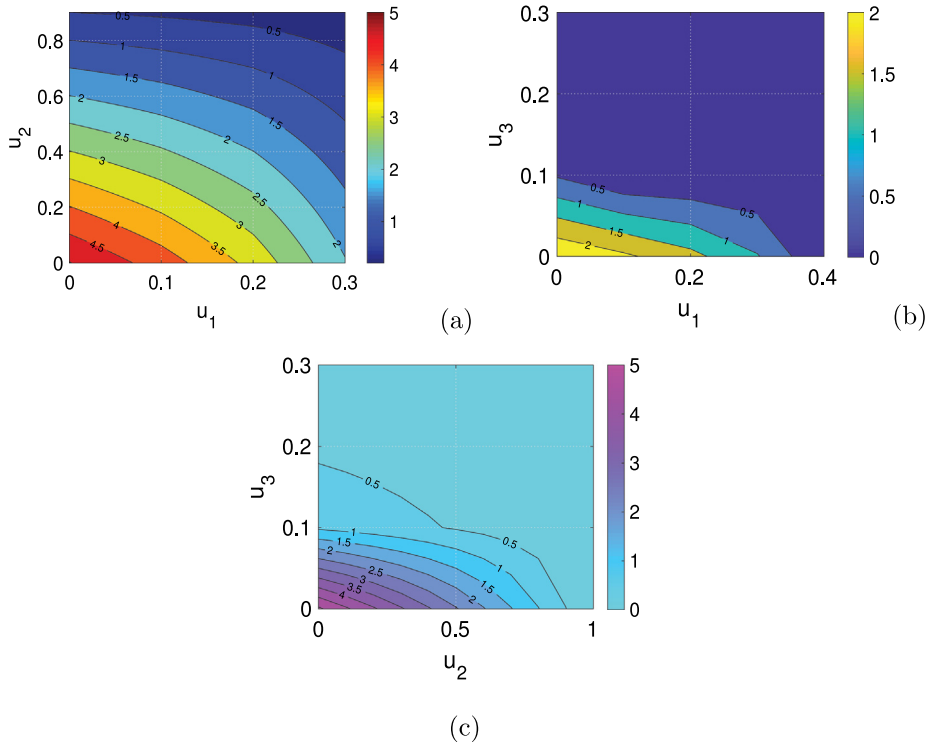
Fig. 6. Contour plots showing the relationship between R_0 and disease control strategies u_i, $i = 1, 2, 3$.

results shows that memory effects have strong influence on predicting the growth and peak of infections. In this scenario, one can observe that as the derivative order q is reduced from 1, the memory effects of the system increase and as a result, infections grow quickly, peak earlier and die over time compared to when the memory effects are reduced.

3. The optimal control problem

To determine an optimal way to control CHIKV during an outbreak, all disease intervention strategies in (7) are now assumed to vary with time, that is., $u_i \rightarrow u_i(t)$, $i = 1, 2, 3$. Using the same variable and parameter names defined earlier, the system of differential equations describing our model with controls is:

$$
\left.
\begin{aligned}
{}^{c}_{b}D^q_t A_v(t) &= f(A_v, N_v) - (\phi^q_v + u_1(t) + d^q_v)A_v, \\
{}^{c}_{b}D^q_t S_v(t) &= \phi^q_v A_v - \frac{b^q_v \beta_h (1 - u_2(t))(I_{hs} + I_{ha})}{N_h} S_v - (u_3(t) + \mu^q_v)S_v, \\
{}^{c}_{b}D^q_t E_v(t) &= \frac{b^q_v \beta_h (1 - u_2(t))(I_{hs} + I_{ha})}{N_h} S_v - (\alpha^q_v + u_3(t) + \mu^q_v)E_v, \\
{}^{c}_{b}D^q_t I_v(t) &= \alpha^q_v E_v - (u_3(t) + \mu^q_v)I_v, \\
{}^{c}_{b}D^q_t S_h(t) &= -\frac{b^q_v(1 - u_2(t))\beta_v I_v}{N_h} S_h, \\
{}^{c}_{b}D^q_t E_h(t) &= \frac{b^q_v(1 - u_2(t))\beta_v I_v}{N_h} S_h - \alpha^q_h E_h, \\
{}^{c}_{b}D^q_t I_{hs}(t) &= (1 - f_h)\alpha^q_h E_h - \gamma^q_h I_{hs}, \\
{}^{c}_{b}D^q_t I_{ha}(t) &= f_h \alpha^q_h E_h - \delta^q_h I_{ha}, \\
{}^{c}_{b}D^q_t R_h(t) &= \gamma^q_h I_{hs} + \delta^q_h I_{ha}.
\end{aligned}
\right\}
\tag{12}
$$

A successful control strategy is one that minimizes the number of infected individuals at minimal implementation costs. Thus, our goal is to find a treble of controls (u^*_1, u^*_2, u^*_3) that minimize the number of infected humans and the cost of implementing the
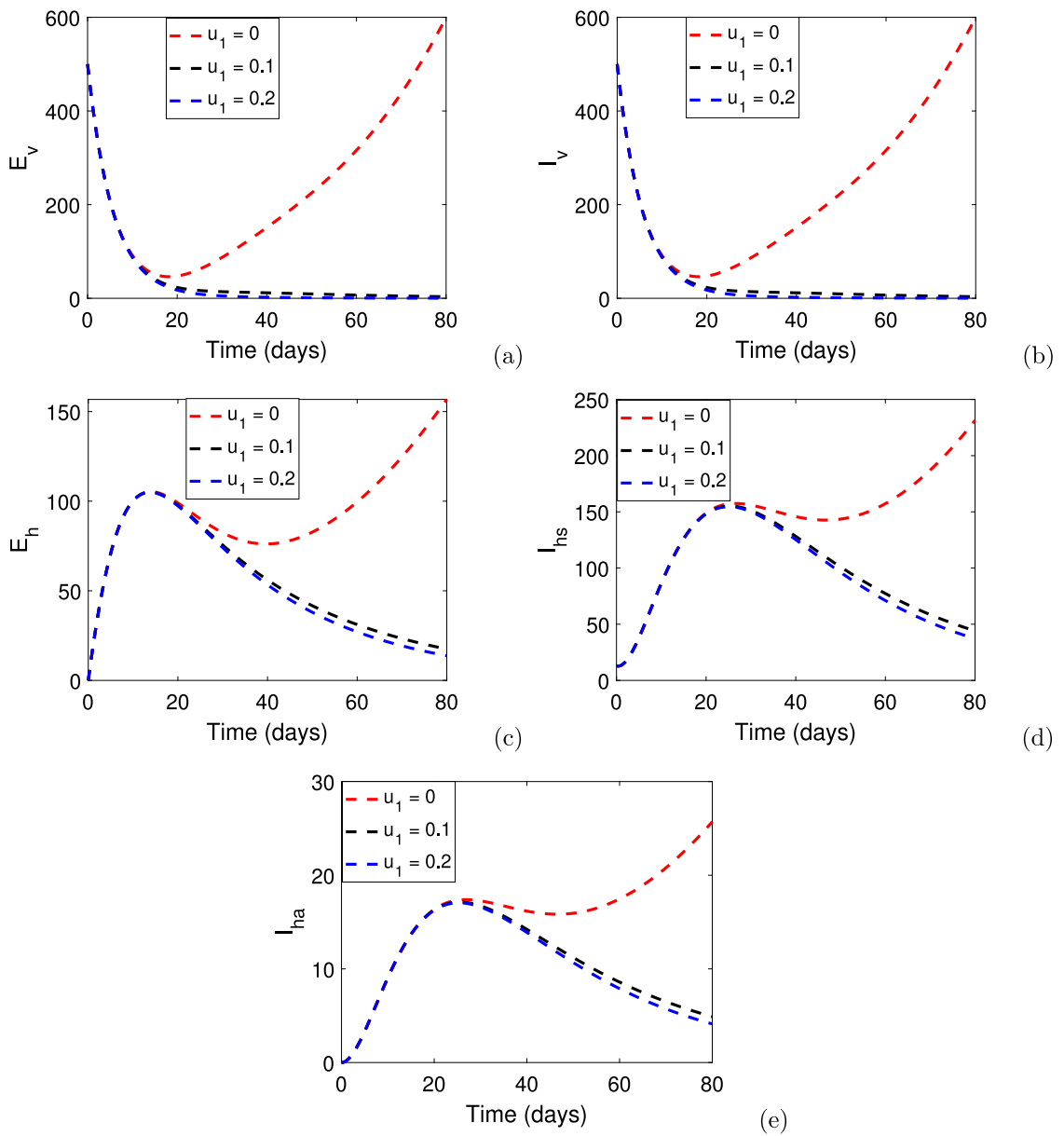
Fig. 7. Effects of varying u_1 on vector and host population dynamics over time.
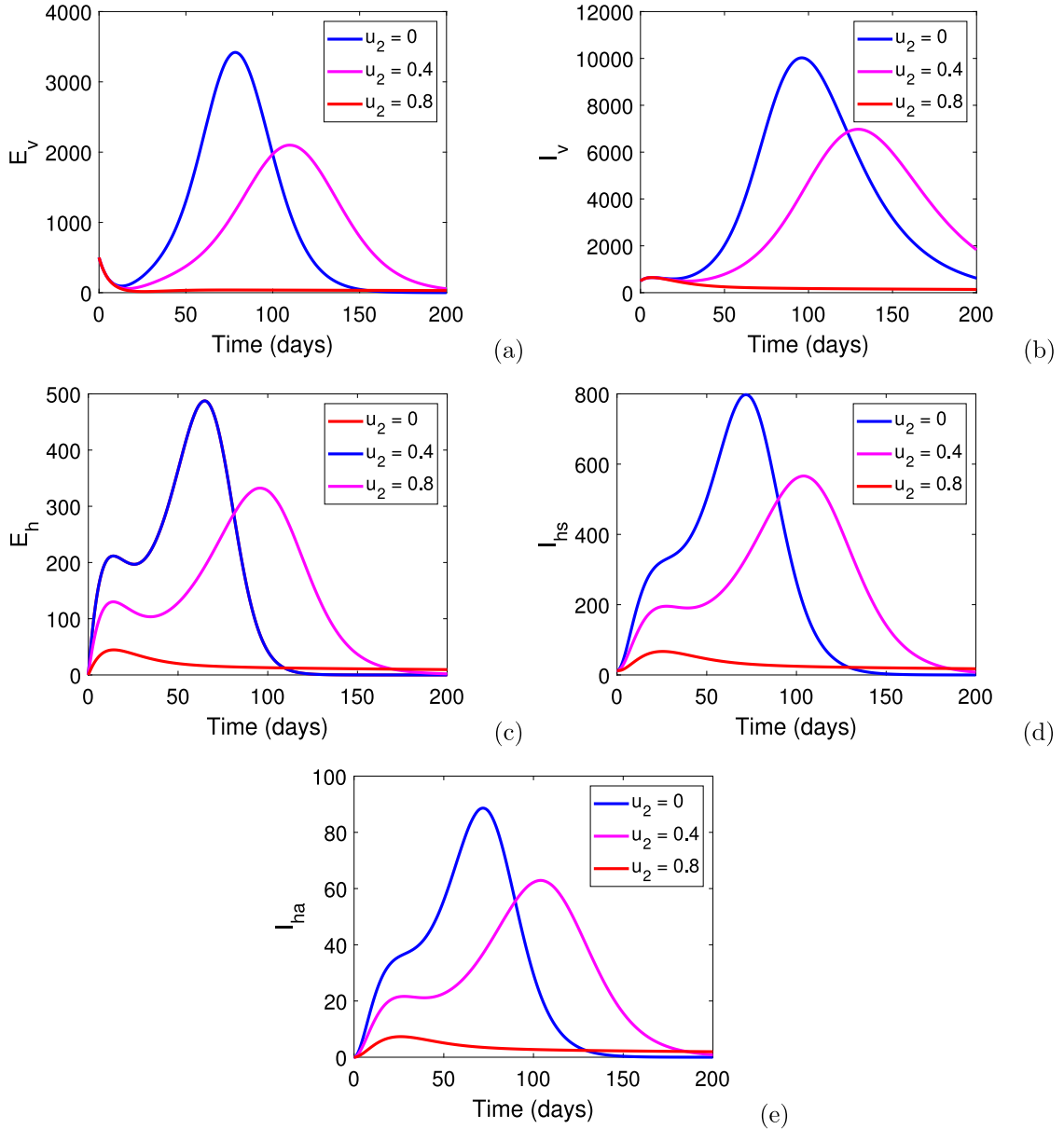
Fig. 8. Effects of varying u_2 on vector and host population dynamics over time.

controls. Mathematically, we propose the following objective functional:

$$J(u_1(t), u_2(t), u_3(t)) = \int_0^T \left[I_{hs}(t) + I_{ha}(t) + \frac{W_1}{2} u_1^2(t) + \frac{W_2}{2} u_2^2(t) + \frac{W_3}{2} u_3^2(t) \right] dt, \qquad (13)$$

where W_1, W_2 and W_3 are positive constants meant to transfer the integral into monetary quantity over a finite horizon $[0, T]$. One can observe that the proposed objective functional is nonlinear-quadratic that a quadratic structure in the control has mathematical advantages. For example the control set is a compact and convex, it follows that the Hamiltonian attains its minimum over the control set at a unique point. We seek the treble $(u_1^*, u_2^*, u_3^*) \in U$ such that:

$$J(u_1^*, u_2^*, u_3^*) = \inf_{(u_1, u_2, u_3) \in U} J(u_1, u_2, u_3), \qquad (14)$$

for the admissible set $U = \{(u_1, u_2, u_3) \in (L^\infty(0, T))^3 : 0 \le u_i \le u_{i\max}, u_{i\max} \in \mathbb{R}^+, i = 1, 2, 3\}$.
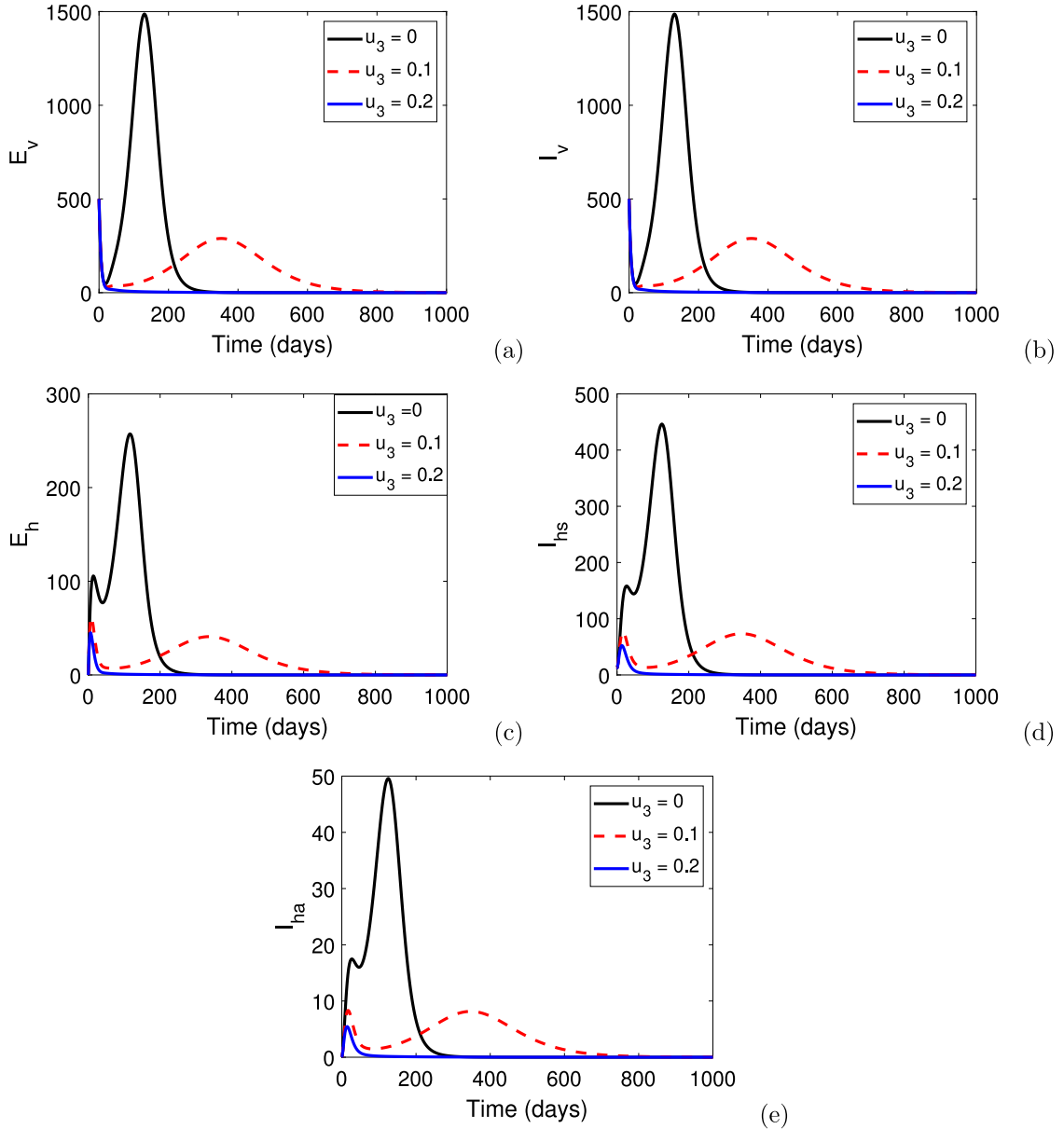
Fig. 9. Effects of varying u_3 on vector and host population dynamics over time.

Making use of the Pontryagin Maximum principle [30], we now reformulate the problem to determine the optimal control variables $(u_1(t), u_2(t), u_3(t))$, such that condition (14) with constrained model (12) is equivalent to the problem of minimizing the Hamiltonian:

$$H(t) = I_{hs} + I_{ha} + \frac{W_1}{2}u_1^2 + \frac{W_2}{2}u_2^2 + \frac{W_3}{2}u_3^2 + \sum_{j=i}^{9} \lambda_j g_j(u_1, u_2, u_3, \Psi),$$ (15)

where $g_j(u_1, u_2, u_3, \Psi)$ is the right-hand side of the differential equation of the jth state variable, from system (11), with $\Psi = \{A_v, S_v, E_v, I_v, S_h, E_h, I_{hs}, I_{ha}\}$. From (13) and (15), the necessary conditions for Fractional optimal control problems (FOCPs) are given as follows [31]:

$$_{t_0}^{c}D_t^q \lambda_j = \frac{\partial H}{\partial \Psi_k}, \qquad j = 1, 2, 3, 4, \ldots, 8, 9. \quad \Psi_k = \{A_v, S_v, E_v, I_v, S_h, E_h, I_{hs}, I_{ha}\},$$
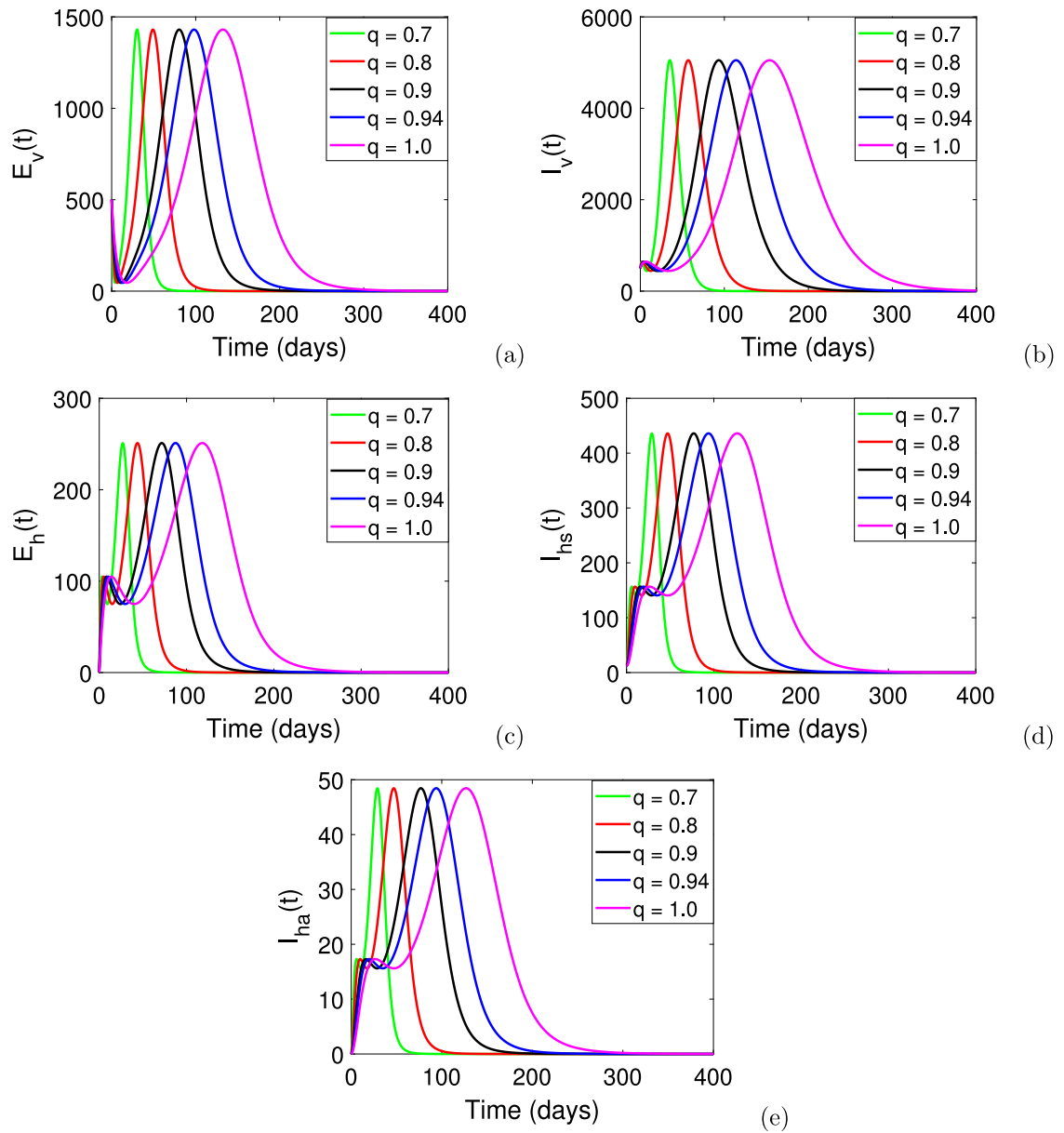
Fig. 10. Dynamical solutions of model (7) with different fractional order derivatives, $q = \{0.7, 0.8, 0.94, 1.0\}$. All the model parameters assumed parameter values in Table 1.

$$0 = \frac{\partial H}{\partial u_i}, \qquad i = 1, 2, 3,$$

$${}_{t_0}^{c} D_t^q \Psi_k = \frac{\partial H}{\partial \lambda_j},$$

$$\lambda_j(T) = 0, \qquad j = 1, 2, 3, 4, \dots, 8, 9.$$

Therefore, given an optimal control treble (u_1^*, u_2^*, u_3^*) and solutions $(A_v, S_v, E_v, I_v, S_h, E_h, I_{hs}, I_{ha})$, of the corresponding states system (12), there exist adjoint functions λ_j, $j = 1, 2, 3, 4, \dots, 9$, satisfying:

$$
\left.
\begin{aligned}
{}_{t_0}^{c} D_t^q \lambda_1 &= -\lambda_1 \left(\phi_v^q + d_v^q + u_1 + \theta_v^q \frac{N_v}{K_v} \right) + \phi_v^q \lambda_2, \\
{}_{t_0}^{c} D_t^q \lambda_2 &= \left(1 - \frac{A_v}{K_v} \right) \theta_v^q \lambda_1 - (\mu_v^q + u_3) \lambda_2 - \frac{b_v^q \beta_h (1 - u_2)(I_{hs} + I_{ha})}{N_h} (\lambda_2 - \lambda_3), \\
{}_{t_0}^{c} D_t^q \lambda_3 &= \left(1 - \frac{A_v}{K_v} \right) \theta_v^q \lambda_1 - (\alpha_v^q + u_3 + \mu_v^q) \lambda_3 + \alpha_v^q \lambda_4, \\
{}_{t_0}^{c} D_t^q \lambda_4 &= \left(1 - \frac{A_v}{K_v} \right) \theta_v^q \lambda_1 - (\mu_v + u_3^q) \lambda_4 - \frac{b_v^q \beta_v (1 - u_2) S_h}{N_h} (\lambda_5 - \lambda_6), \\
{}_{t_0}^{c} D_t^q \lambda_5 &= -\frac{b_v^q \beta_v (1 - u_2) I_v}{N_h} (\lambda_5 - \lambda_6), \\
{}_{t_0}^{c} D_t^q \lambda_6 &= -\alpha_h^q \lambda_6 + (1 - f_h) \alpha_h^q \lambda_7 + f_h \alpha_h^q \lambda_8, \\
{}_{t_0}^{c} D_t^q \lambda_7 &= 1 - \frac{b_v^q \beta_h (1 - u_2) S_v}{N_h} (\lambda_2 - \lambda_3) - \gamma_h (\lambda_7 - \lambda_9), \\
{}_{t_0}^{c} D_t^q \lambda_8 &= 1 - \frac{b_v^q \beta_h (1 - u_2) S_v}{N_h} (\lambda_2 - \lambda_3) - \delta_h^q (\lambda_8 - \lambda_9), \\
{}_{t_0}^{c} D_t^q \lambda_9 &= 0,
\end{aligned}
\right\}
\tag{16}
$$

with transversality conditions $\lambda_j(T) = 0$. Furthermore, the optimal controls are characterized by the optimality conditions:

$$
\left.
\begin{aligned}
u_1 &= \min\left\{ u_{1\max}, \max\left\{ 0, \frac{A_v \lambda_1}{W_1} \right\} \right\}, \\
u_2 &= \min\left\{ u_{2\max}, \max\left(0, \frac{b_v^q \beta_h (I_{hs} + I_{ha})(\lambda_3 - \lambda_2) S_v}{W_2 N_h} + \frac{b_v^q \beta_v I_v S_h (\lambda_6 - \lambda_5)}{W_2 N_h} \right) \right\}, \\
u_3 &= \min\left\{ u_{3\max}, \max\left(0, \frac{\lambda_2 S_v + \lambda_3 E_v + \lambda_4 I_v}{W_3} \right) \right\}.
\end{aligned}
\right\}
\tag{17}
$$

3.1. Optimal control numerical results

In this section, we present numerical solutions of model (12). The solutions were determined by solving model (12) using an optimization algorithm, forward–backward sweep method [31,32]. In carrying out the simulations, we assumed that the cost of chemical vector control (larvicide spraying and insecticides) is higher than that of using physical barriers. Based on this assertion, we set $(W_1 = W_3) > W_2$, that is., the cost incurred through efforts u_1 and u_3 are considered equivalent but higher than those associated with control u_2. Furthermore, we consider the following strategies and examine the corresponding outcomes numerically: (i) **Strategy A:** Use of physical barriers alone, that is., $u_1(t) = u_3(t) = 0$ and $u_2(t) \neq 0$. (ii) **Strategy B:** Use of both physical barriers and chemical control, that is., $u_1(t) \neq 0$, $u_3(t) \neq 0$, and $u_2(t) \neq 0$.

Strategy A: Use of physical barriers alone

Prior studies on vector-borne diseases (such as CHIKV and malaria) transmitted by mosquitoes have shown that physical barriers such as insecticide-treated bednets (ITNs) or wearing of loose-fitting long-sleeved shirts and long pants are effective in minimizing human and vector contact, thereby reducing chances of transmission and spread of vector borne diseases (VBDs) [33]. Most importantly, the use of physical barriers to mitigate the spread of VBDs comes handy in resource-limited settings where the host population cannot afford to purchase insecticides. Prior studies have also shown that on average the cost of a single bednet is between USD 2.2 and USD 4.7 [34]. Based on these results, we set $W_2 = 4.7$ (Fig. 11).

Under Strategy A, the optimal control strategy significantly reduces the number of infected host and vector populations (compared to the case without control) over time. In particular, the control strategy will avert approximately 2492 infections (in the human population) over the entire time horizon (100 days) at a total cost of USD 3108.3.

In Fig. 11 (f), we can observe that the control profile of $u_2(t)$ starts at its maximum ($u_2 = 0.85$) and remains there until the end. This implies that to achieve the desired outcome control $u_2(t)$, needs to be maintained to its maximum capacity nearly until the end. Considering the complexity of the maintaining a control effort at its maximum intensity over a 100 day period, one can conclude that use of physical barriers alone may have some challenges with regards to quick elimination of CHIKV during an outbreak. Hence, it may be worth to couple it with other strategies.
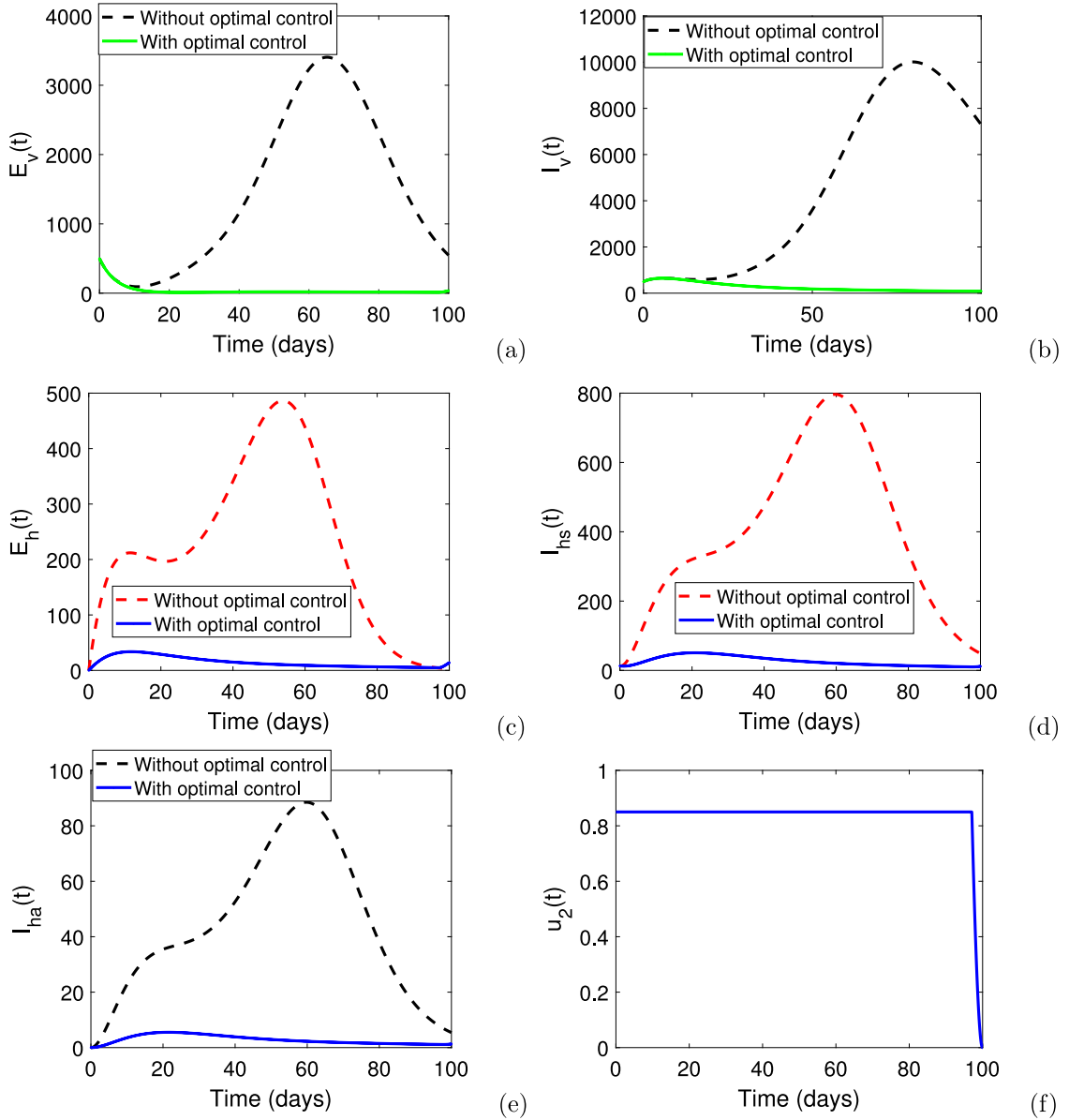
Fig. 11. Simulation results for Strategy A (no larvicide $u_1 = 0$ and insecticide use $u_3 = 0$) over time, with $q = 0.94$, $T = 29.5\ °C$, $u_2 = 0.85$.

Strategy B: Use of both physical barriers and chemical control

We quantitatively and qualitatively explore the use of both physical barriers and chemical control (larvicides and insecticides) to minimize CHIKV transmission during an outbreak (Fig. 12). Since the cost of vector control through chemicals is known to be higher relative to that of physical barriers, we assume that $(W_1 = W_3) \geq nW_2$, where $n \geq 1$. Moreover, since the extensive use of chemical is associated with significant environmental challenges we will consider their use at low intensity, that is., $(u_{1\max}, u_{3\max}) < u_{2\max} < 1$. When all the aforementioned intervention strategies (larvicides, physical barriers and insecticides) are in use and time-dependent, we note that the disease will be eliminated in the community within a period of about 50 days (Fig. 12). Precisely, strategy B will avert approximately 4168 infections with a total cost of USD $J = 1988.9$ and the associated ACER for this strategy is 0.4851. In Fig. 12(f), we observe that all three control profiles start from their respective maxima, however, after about 50,60 and 90 days, the control profile of u_2, u_1 and u_3 respectively to their minima. This suggests that use of physical barriers, larvicides and insecticides may be relaxed or ceased after 50, 60 and 90 days, respectively. Comparing the two strategies, A and B, one can note that strategy B is more effective since more infections will averted over time at less cost in relative to strategy A. Precisely, the average cost-effectiveness ratio (ACER) (18) of strategy B is 0.48 while that of strategy A is 1.25. The average cost-effectiveness
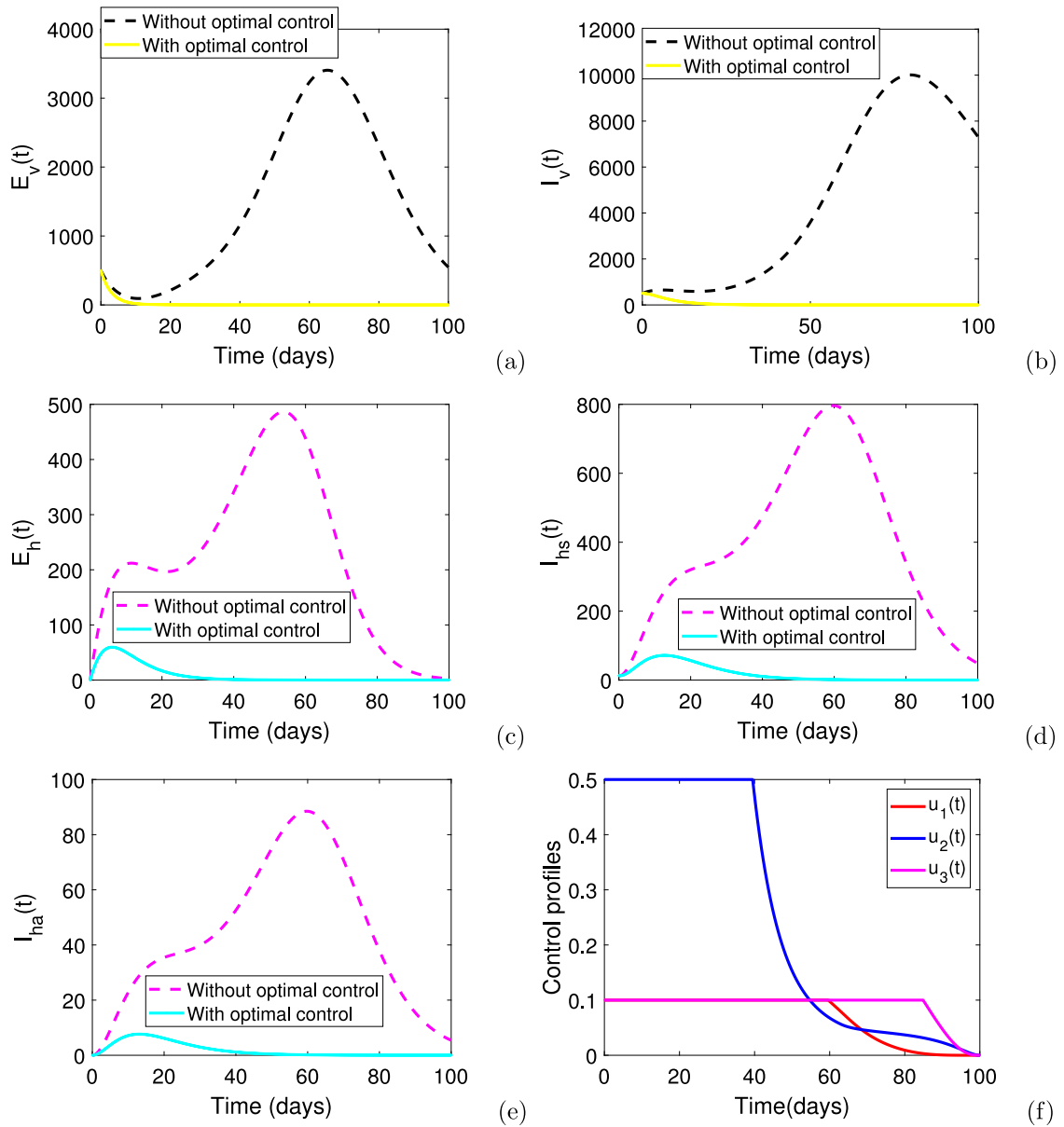
Fig. 12. Simulation results for Strategy B over time, with $q = 0.94$, $T = 29.5$ °C, $n = 2$, $u_{1max} = u_{3max} = 0.1$ and $u_{2max} = 0.5$.

ratio (ACER) is defined by:

$$\text{ACER} = \frac{\text{Cost produced by the intervention}}{\text{Number of infection averted}}, \tag{18}$$

Reducing the intensity of chemical usage by 50% and increasing the intensity of physical barriers from 0.5 to 0.6, will increase the duration in which all three controls need to be maintained at their maximum capacity before being relaxed or ceased (Fig. 13). In particular, control u_1 and u_2 may be relaxed after 80 days, which is approximately 20 days later than when their intensities are at $u_{1max} = 0.1$ and $u_{2max} = 0.5$. In addition, with high costs, we observed that the number of infections reduced over the entire time horizon reduces significantly (Table 2).

4. Conclusions and discussion

This paper proposes a fractional order model for CHIKV transmission that incorporates temperature effects and three disease control strategies; larvicide use, insecticide use and usage of physical barrier. The proposed model was calibrated based on data
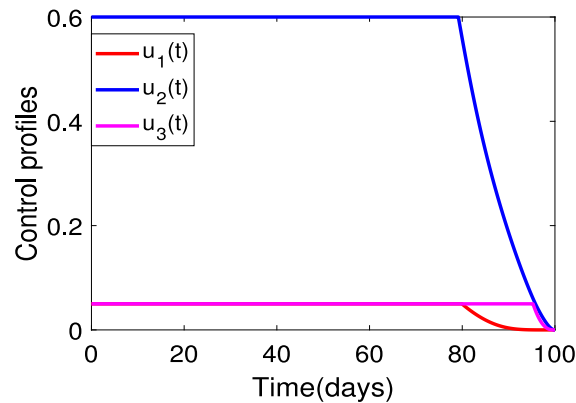
Fig. 13. Simulation results for Strategy B over time, with $q = 0.94$, $T = 29.5$ °C, $n = 2$, $u_{1max} = u_{3max} = 0.05$ and $u_{2max} = 0.6$.

Table 2
Effects of costs of implementation on infections averted.

n	Total cost (J)	Infections averted	ACER
2	1988.9	4168	0.477
5	2120.2	4156	0.510
10	2253.5	4128	0.546

from literature and validated with daily chikungunya fever cases reported at Kadmat primary health centre from 2 July to 30 August 2007. Through data fitting, it was observed that memory effects have an influence on modelling the spread of CHIKV and model predictions with fractional order $q = 0.94$ gave better estimates compared model predictions with the classical model (the integer differential order model). We computed the basic reproduction number R_0 and investigate its sensitivity to model parameters using the partial rank correlation coefficient method. We observed that all the proposed intervention strategies have a significant impact on reducing the size of R_0. In particular, we observed that an increase in insecticide use by 10% will reduce R_0 by 7.8%. Meanwhile, we extended the basic model into an optimal problem where we investigated the impacts of time-dependent deployment of larvicide, insecticide and physical barriers. An important result of this analysis is that deploying all the aforementioned intervention strategies would be a cost effective way to minimize the number of infected humans during CHIKV outbreak. Overall, this work demonstrates the significance of optimal control theory as a tool to suggest management strategies in disease outbreaks.

Finally, this study is not exhaustive, one can extend the proposed model by incorporating biological control. In particular, the extensive use of chemicals to control vectors can lead to insect resistance which has negative effects on effective disease management outcome. Vector control through the use of chemicals may also result adverse in environmental effects. Taking all these into consideration biological control may be incorporated in the proposed model.

CRediT authorship contribution statement

Eva Lusekelo: Formal analysis, Methodology. **Mlyashimbi Helikumi:** Supervision, Writing – review & editing. **Dmitry Kuznetsov:** Supervision, Writing – review & editing. **Steady Mushayabasa:** Supervision, Writing – review & editing.

Declaration of competing interest

The authors declare that they have no known competing financial interests or personal relationships that could have appeared to influence the work reported in this paper.

Data availability

Data link has be included in the document

Acknowledgements

References

[1] Kumar MS, Kamaraj P, Khan SA, Allam RR, Barde PV, Dwibedi B, Kanungo S, Mohan U, Mohanty SS, Roy S, et al. Seroprevalence of chikungunya virus infection in India, 2017: a cross-sectional population-based serosurvey. Lancet Microbe 2021;2(1):e41–7.

[2] Morgan J, Strode C, Salcedo-Sora JE. Climatic and socio-economic factors supporting the co-circulation of dengue, Zika and chikungunya in three different ecosystems in Colombia. PLoS Negl Trop Dis 2021;15(3):e0009259.

[3] Mordecai EA, Cohen JM, Evans MV, Gudapati P, Johnson LR, Lippi CA, Miazgowicz K, Murdock CC, Rohr JR, Ryan SJ, et al. Detecting the impact of temperature on transmission of Zika, dengue, and chikungunya using mechanistic models. PLoS Negl Trop Dis 2017;11(4):e0005568.

[4] Bellone R, Failloux A-B. The role of temperature in shaping mosquito-borne viruses transmission. Front Microbiol 2020;2388.

[5] Huber JH, Childs ML, Caldwell JM, Mordecai EA. Seasonal temperature variation influences climate suitability for dengue, chikungunya, and Zika transmission. PLoS Negl Trop Dis 2018;12(5):e0006451.

[6] Kakarla SG, Mopuri R, Mutheneni SR, Bhimala KR, Kumaraswamy S, Kadiri MR, Gouda KC, Upadhyayula SM. Temperature dependent transmission potential model for chikungunya in India. Sci Total Environ 2019;647:66–74.

[7] Lusekelo E, Helikumi M, Kuznetsov D, Mushayabasa S. Modeling the effects of temperature and heterogeneous biting exposure on chikungunya virus disease dynamics. Inf Med Unlocked 2022;101007.

[8] Zhu G, Liu T, Xiao J, Zhang B, Song T, Zhang Y, Lin L, Peng Z, Deng A, Ma W, et al. Effects of human mobility, temperature and mosquito control on the spatiotemporal transmission of dengue. Sci Total Environ 2019;651:969–78.

[9] Liu X, Wang Y, Zhao X-Q. Dynamics of a climate-based periodic Chikungunya model with incubation period. Appl Math Model 2020;80:151–68.

[10] Helikumi M, Eustace G, Mushayabasa S. Dynamics of a fractional-order chikungunya model with asymptomatic infectious class. Comput Math Methods Med 2022;2022.

[11] Abidemi A, Fatoyinbo HO, Asamoah JKK, Muni SS. Evaluation of the efficacy of wolbachia intervention on dengue burden in a population: A mathematical insight. In: 2022 International conference on decision aid sciences and applications (DASA). IEEE; 2022, p. 1618–27.

[12] Helikumi M, Kgosimore M, Kuznetsov D, Mushayabasa S. A fractional-order Trypanosoma brucei rhodesiense model with vector saturation and temperature dependent parameters. Adv Difference Equ 2020;2020(1):1–23.

[13] Baleanu D, Abadi MH, Jajarmi A, Vahid KZ, Nieto J. A new comparative study on the general fractional model of COVID-19 with isolation and quarantine effects. Alex Eng J 2022;61(6):4779–91.

[14] Gashirai TB, Hove-Musekwa SD, Mushayabasa S. Dynamical analysis of a fractional-order foot-and-mouth disease model. Math Sci 2021;15(1):65–82.

[15] Chatterjee AN, Basir FA, Ahmad B, Alsaedi A. A fractional-order compartmental model of vaccination for COVID-19 with the fear factor. Mathematics 2022;10(9):1451.

[16] Daudi S, Luboobi L, Kgosimore M, Kuznetsov D, Mushayabasa S. A mathematical model for fall armyworm management on maize biomass. Adv Difference Equ 2021;2021(1):1–27.

[17] Kam Y-W, Lee WW, Simarmata D, Harjanto S, Teng T-S, Tolou H, Chow A, Lin RT, Leo Y-S, Rénia L, et al. Longitudinal analysis of the human antibody response to Chikungunya virus infection: implications for serodiagnosis and vaccine development. J Virol 2012;86(23):13005–15.

[18] Podlubny I. Fractional differential equations: an introduction to fractional derivatives, fractional differential equations, to methods of their solution and some of their applications. Elsevier; 1998.

[19] Yang H, Macoris M, Galvani M, Andrighetti M, Wanderley D. Assessing the effects of temperature on the population of Aedes aegypti, the vector of dengue. Epidemiol Infect 2009;137(8):1188–202.

[20] Lambrechts L, Paaijmans KP, Fansiri T, Carrington LB, Kramer LD, Thomas MB, Scott TW. Impact of daily temperature fluctuations on dengue virus transmission by Aedes aegypti. Proc Natl Acad Sci 2011;108(18):7460–5.

[21] Scott TW, Amerasinghe PH, Morrison AC, Lorenz LH, Clark GG, Strickman D, Kittayapong P, Edman JD. Longitudinal studies of Aedes aegypti (Diptera: Culicidae) in Thailand and Puerto Rico: blood feeding frequency. J Med Entomol 2000;37(1):89–101.

[22] Van den Driessche P, Watmough J. Reproduction numbers and sub-threshold endemic equilibria for compartmental models of disease transmission. Math Biosci 2002;180(1–2):29–48.

[23] Sharma R, Ali SM, Dhillon G. Epidemiological and entomological aspects of an outbreak of chikungunya in Lakshadweep Islands, India, during 2007. 2008.

[24] Nelder JA, Mead R. A simplex method for function minimization. Comput J 1965;7(4):308–13.

[25] Gashirai TB, Hove-Musekwa SD, Mushayabasa S. Optimal control applied to a fractional-order foot-and-mouth disease model. Int J Appl Comput Math 2021;7(3):1–24.

[26] Chinyoka M, Gashirai TB, Mushayabasa S. On the dynamics of a fractional-order ebola epidemic model with nonlinear incidence rates. Discrete Dyn Nat Soc 2021;2021.

[27] Feng X, Huo X, Tang B, Tang S, Wang K, Wu J. Modelling and analyzing virus mutation dynamics of chikungunya outbreaks. Sci Rep 2019;9(1):1–15.

[28] Marino S, Hogue IB, Ray CJ, Kirschner DE. A methodology for performing global uncertainty and sensitivity analysis in systems biology. J Theoret Biol 2008;254(1):178–96.

[29] Mushayabasa S, Bhunu C, et al. Assessing the impact of educational campaigns on controlling HCV among women in prison settings. Commun Nonlinear Sci Numer Simul 2012;17(4):1714–24.

[30] á Pontryagin L, et al. The mathematical theory of optimal processes. 1962.

[31] Kheiri H, Jafari M. Optimal control of a fractional-order model for the HIV/AIDS epidemic. Int J Biomath 2018;11(07):1850086.

[32] Lenhart S, Workman JT. Optimal control applied to biological models. Chapman and Hall/CRC; 2007.

[33] Che-Mendoza A, Medina-Barreiro A, Koyoc-Cardeña E, Uc-Puc V, Contreras-Perera Y, Herrera-Bojórquez J, Dzul-Manzanilla F, Correa-Morales F, Ranson H, Lenhart A, et al. House screening with insecticide-treated netting provides sustained reductions in domestic populations of Aedes aegypti in Merida, Mexico. PLoS Negl Trop Dis 2018;12(3):e0006283.

[34] Pulkki-Brännström A-M, Wolff C, Brännström N, Skordis-Worrall J. Cost and cost effectiveness of long-lasting insecticide-treated bed nets-a model-based analysis. Cost Eff Resour Allocation 2012;10(1):1–13.